

# Efficient Metal-Free Electrocatalysts for Oxygen Reduction: Polyaniline-Derived N- and O-Doped Mesoporous Carbons

Rafael Silva,<sup>†</sup> Damien Voiry,<sup>‡</sup> Manish Chhowalla,<sup>‡</sup> and Tewodros Asefa<sup>\*,†,§</sup>

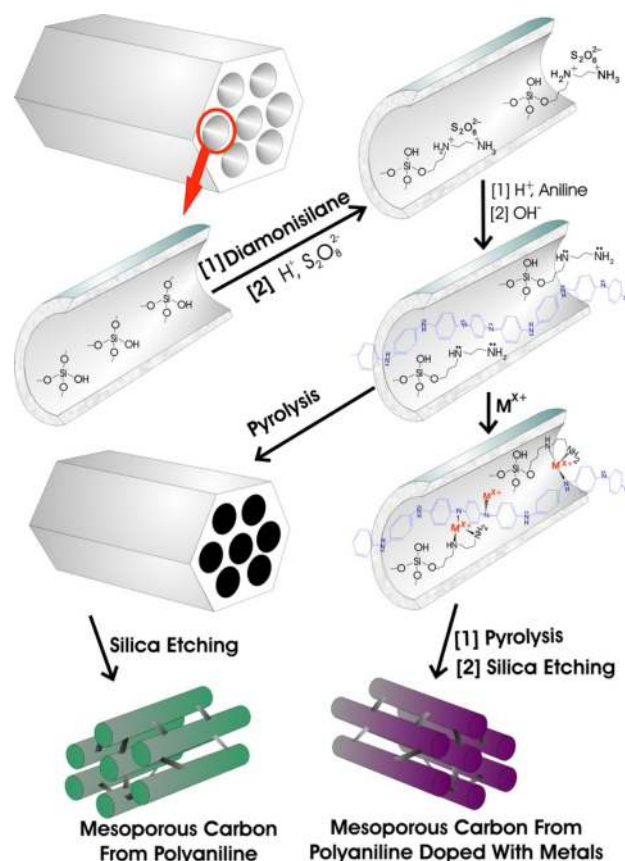
<sup>†</sup>Department of Chemistry and Chemical Biology, <sup>‡</sup>Department of Materials Science and Engineering, and <sup>§</sup>Department of Chemical and Biochemical Engineering, Rutgers, The State University of New Jersey, Piscataway, New Jersey 08854, United States

**S** Supporting Information

**ABSTRACT:** The oxygen reduction reaction (ORR)—one of the two half-reactions in fuel cells—is one of the bottlenecks that has prevented fuel cells from finding a wide range of applications today. This is because ORR is inherently a sluggish reaction; it is also because inexpensive and sustainable ORR electrocatalysts that are not only efficient but also are based on earth-abundant elements are hard to come by. Herein we report the synthesis of novel carbon-based materials that can contribute to solving these challenges associated with ORR. Mesoporous oxygen- and nitrogen-doped carbons were synthesized from *in situ* polymerized mesoporous silica-supported polyaniline (PANI) by carbonization of the latter, followed by etching away the mesoporous silica template from it. The synthetic method also allowed the immobilization of different metals such as Fe and Co easily into the system. While all the resulting materials showed outstanding electrocatalytic activity toward ORR, the metal-free, PANI-derived mesoporous carbon (dubbed PDMC), in particular, exhibited the highest activity, challenging conventional paradigms. This unprecedented activity by the metal-free PDMC toward ORR was attributed to the synergistic activities of nitrogen and oxygen (or hydroxyl) species that were implanted in it by PANI/mesoporous silica during pyrolysis.

In the face of global problems associated with the lack of sustainable and renewable energy sources as well as environmental pollution caused by fossil fuels, fuel cells—which can generate electricity from fuels such as hydrogen—have long been considered among the possible solutions to these problems.<sup>1</sup> Unfortunately, there are currently two bottlenecks preventing fuel cells from finding a wide range of applications. The first is that the electrodes (both cathode and anode) in many conventional fuel cells contain electrocatalysts composed of unsustainable materials or expensive and less earth-abundant noble metals such as platinum. The second problem is the inherently poor efficiency of the oxygen reduction reaction (ORR)—one of the two redox (half) reactions taking place in fuel cells. Even with platinum-based electrodes or electrocatalysts, this reaction is very sluggish or has overpotentials as high as 500–600 mV [cf. the second half-reaction, i.e., the hydrogen oxidation reaction on the anode side of fuel cells, which typically occurs with overpotentials as low as 50 mV].<sup>2</sup> The ORR is, therefore, mainly responsible for the limited current density

**Scheme 1. Synthesis of N- and O-Doped Mesoporous Carbons with or without Metal Dopants by Carbonization of PANI/SBA-15, Followed by Etching SBA-15**



and lower cell voltages typically obtained from conventional fuel cells today. Thus, a massive improvement in fuel cells requires not only development of electrocatalysts based on sustainable and earth-abundant elements (e.g., noble metal-free electrocatalysts) but also rational design and synthesis of electrocatalysts capable of performing ORR as efficiently as, if not better than, platinum.

Recent efforts to obtain replacements for platinum and its congener metals for ORR have resulted in some new contenders, including some N-doped carbon-based materials.<sup>3</sup> These and

Received: March 8, 2013

other recent studies have also suggested that further improvements in the catalytic activities of carbon-based materials could be achieved by doping the carbon with heteroatoms such as boron, phosphorus, or sulfur.<sup>4</sup> The mechanisms by which such heteroatoms improve the electrocatalytic activities of carbons in ORR and the exact functions of the heteroatoms in these systems are not yet well-understood, though. Besides nonmetals, metals—mainly cobalt ions—have also been used as dopants to improve the electrocatalytic activity of N-doped carbon-based materials. Although some authors suggested that the metal ions that remain coordinated to the N atoms of the N-doped carbons act as the active sites for ORR,<sup>5</sup> other recent studies suggested otherwise.<sup>6</sup> Regardless of the mechanism, metal-containing catalysts are still less preferable for ORR because the acidic or basic media often used for ORR can make many metals leach from the electrodes' (electrocatalysts') surfaces over time, making the system lose its electrocatalytic activity as well as shelf life.<sup>7</sup> Therefore, the development of nonmetallic heteroatom-doped multifunctional carbon-based materials that can show superior activity toward ORR is warranted.

Herein we report the synthesis of novel, metal-free polyaniline (PANI)-derived N- and O-doped mesoporous carbons (PDMCs), which can efficiently catalyze ORR with higher current density and lower overpotential compared with the commercially used Pt/C electrocatalyst. The material was synthesized by polymerizing PANI *in situ* within the pores of SBA-15 mesoporous silica, followed by subjecting PANI/SBA-15 to carbonization under an inert atmosphere, and finally etching away the silica framework, as illustrated in Scheme 1. The corresponding metal-containing PDMCs were easily synthesized by immobilizing different metal ions such as Fe(II) and/or Co(II) into the PANI/SBA-15 before pyrolysis.

Polymerization of PANI within the pores of SBA-15 was carried out as we reported previously.<sup>8</sup> As shown in Scheme 1, first the internal channel walls of SBA-15 were selectively functionalized with alkyldiaminosilane. The alkyldiamine groups were then converted into ammonium ions using aqueous HCl solution. The resulting alkylammonium ions were used to anchor persulfate ions that were, in turn, used to oxidize and initiate the polymerization of aniline into PANI *in situ* within the pores of SBA-15 (see Supporting Information for details). This produced PANI/SBA-15. The amine groups in PANI/SBA-15 were utilized for immobilization of different metal ions homogeneously throughout the pores of the PANI/SBA-15; this was easily achieved by stirring PANI/SBA-15 with aqueous solutions containing various metal salts. Finally, upon carbonization of the resulting PANI/SBA-15 material or its metal ion-doped counterparts, followed by etching away the SBA-15 hard template, different PDMC materials, metal-free or with metals, respectively, were obtained.

We chose PANI as precursor for making the N-doped mesoporous carbons owing to its high N/C atomic ratio (0.167) and high molar weight, which prevents its vaporization at high temperatures. Conversely, even when not under a nitrogen-rich atmosphere, the pyrolysis of PANI can result in N-doped carbons with high N content,<sup>10</sup> and possibly better electrocatalytic activity. Furthermore, by confining PANI within the thermally robust nanosized cavities of SBA-15 and pyrolyzing the resulting material, we hoped that we would obtain N-doped carbons with not only high surface area but also higher N content, as the SBA-15 could hinder the vaporization of small CN species.<sup>9</sup> The PDMCs we finally obtained had indeed a large amount of N atoms as dopant (see below); this is effected, however, not only

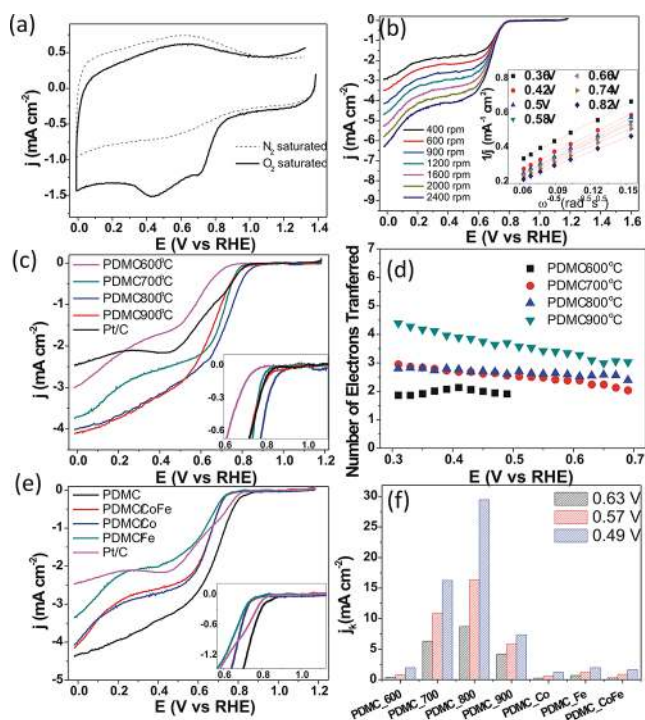


**Figure 1.** (a) Cyclic voltammograms of PDMC synthesized at a pyrolysis temperature of 800 °C (PDMC-800) in O<sub>2</sub>- and N<sub>2</sub>-saturated 0.1 mol/L KOH solutions. (b) Polarization curves at different rotating speeds for PDMC-800 (inset shows the corresponding Koutecky–Levich plots). (c) Polarization curves at 900 rpm of PDMCs synthesized at different temperatures. (d) The number of electrons transferred as a function of potential for PDMCs synthesized at different temperatures. (e) Polarization curves at 900 rpm of different PDMCs with or without metals. (f) Kinetic current density ( $J_k$ ) at different potentials for PDMCs synthesized at different temperatures; note that in the case of PDMC-600, data points that did not give a linear graph or enable calculation of the number of electrons are not included.

because of the confinement of PANI within SBA-15 but also because of the presence of the alkylammonium groups in the PANI/SBA-15. Interestingly, besides N, the PDMC materials so obtained also had a significant amount of O species as dopants (thanks to the oxygen implantation by the mesoporous silica template) and therefore exhibited higher electrocatalytic activity toward ORR (see below). The metals were further added into the PANI/SBA-15 because there was precedent that carbon materials obtained from pyrolysis of metal-containing polymers were better catalyst for ORR,<sup>9,10</sup> although other reports indicated otherwise.<sup>3,6,11</sup>

The PDMC materials synthesized above were characterized by transmission electron microscopy (TEM, Figure S1). The results revealed that the morphology of the materials varied greatly with the synthetic conditions employed to make them, especially the pyrolysis temperatures used to carbonize them. For example, the TEM image of PDMC prepared at 600 °C (PDMC-600) showed well-connected tubular-shaped nanostructures; however, the TEM image of PDMC synthesized at 800 °C (PDMC-800) showed rice-shaped nanoparticles. Further close examination of the TEM images of the latter showed the presence of hierarchical porous structures, akin to the characteristic hexagonal channel-like mesoporous structure of SBA-15.<sup>12</sup> The TEM image of the PDMC obtained from PANI/SBA-15 containing Co<sup>2+</sup> ions at pyrolysis temperature of 800 °C (PDMCCo) consisted of highly organized mesoporous carbon structure. This is consistent with a

previous report which suggested that the addition of metal ions into organic molecular precursors of carbon materials assists with the formation of highly organized carbon nanostructures during carbonization.<sup>9</sup> The formation of distinct microstructures and morphology in the PDMC materials when the pyrolysis temperatures were changed and/or when metal ions were used was confirmed by SEM and N<sub>2</sub> gas adsorption measurements as well (Figures S2–S10).

The electrocatalytic activities of all the PDMC materials were then investigated, and the results are presented in Figures 1 and S11–S18. First, the catalytic activity of the metal-free PDMC was assessed by cyclic voltammetry in 0.1 mol/L KOH solutions saturated with O<sub>2</sub> or N<sub>2</sub> (Figure 1a); quick inspection of the results by comparing the cathodic currents obtained in O<sub>2</sub> and N<sub>2</sub> saturated solutions revealed the presence of an intense oxygen reduction current starting at ~0.94 V (vs RHE). Next up, the catalytic activity and kinetics of all the PDMC materials prepared under different conditions toward ORR were analyzed using a rotating disk electrode (RDE). The results along with the corresponding Koutecky–Levich plots, which were obtained from their polarization curves, are displayed in Figures 1b and S11–S18. The latter showed linear graphs for all the samples, indicating the reactions were first order in a wide potential range. The results (e.g., Figure 1c) further revealed that the catalytic activity of the PDMCs toward ORR was directly dependent on the pyrolysis temperatures used to produce the materials. Among the PDMC materials investigated, PDMC-800 gave the best performance or lowest overpotential toward ORR (Figure 1c).

By using the Koutecky–Levich plots, the number of electrons transferred through the PDMC-catalyzed electrocatalytic reaction was then determined (Figure 1d). The results indicated that the electron transfer number in the reactions was correlated to the pyrolysis temperatures used to make the PDMC materials. For instance, PDMC-800, which gave the lowest overpotential for ORR above, yielded a stable electron transfer number with an average value of 2.66 in the potential range in which it was analyzed. PDMC-600 also gave a stable electron transfer number, but with a value of only ca. 2.0. [Despite its relatively poor catalytic activity for ORR due to its relatively higher overpotential and an onset potential of ~0.71 V vs RHE, this material could still serve as an effective electrocatalyst for H<sub>2</sub>O<sub>2</sub> synthesis because electrocatalysts with electron transfer number of 2.0 were known to be highly selective (ca. 100%) toward H<sub>2</sub>O<sub>2</sub> product.<sup>13</sup>] Generally, higher electron transfer numbers, implying higher selectivity toward total oxygen reduction, were achieved with the PDMCs obtained at higher pyrolysis temperatures. For instance, PDMC-900 gave an electron transfer number between 3.0 and 4.0 in the potential range of 0.3–0.7 V. Notably, the electron transfer number of PDMC-900 was 3.78 at 0.5 V; this suggests that the reaction catalyzed by this material was dominated almost exclusively by a one-step, four-electron pathway.<sup>14</sup>

To investigate if and how the addition of metal dopants affects the electrochemical properties of PDMCs, Co(II) or/and Fe(III) ions were added into PANI/SBA-15 before pyrolysis (Scheme 1). When comparing the polarization curves of the PDMCs synthesized with these different metals at 800 °C with those of the corresponding materials synthesized without, an unexpected result was obtained: in lieu of improvement in electrocatalytic activity typical in many carbon-based materials upon doping with metals,<sup>5,6</sup> the ORR signals of the metal-doped PDMCs shifted rather to lower potential (or gave lower overpotentials) compared with that of the metal-free PDMC (Figure 1e).

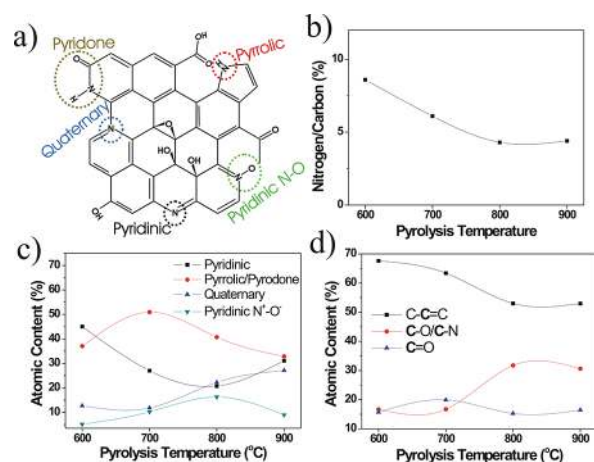


**Figure 2.** (a) Schematic representation of the different N-based functional groups detected on the metal-free PDMC by XPS. (b) N/C atomic ratios, determined by XPS, versus pyrolysis temperature. (c) Atomic %N versus pyrolysis temperature. (d) Atomic %C versus pyrolysis temperature.

Conversely, the metal-free PDMC exhibited the highest electrocatalytic activity. This can also be seen from its significantly higher  $J_k$  (i.e., kinetic current density determined from RDE data), compared with those of the other materials (Figure 1f; see also Supporting Information). The results clearly demonstrate the exceptionally high current density generated in the reaction catalyzed by the metal-free PDMC compared with those catalyzed by PDMCs prepared with Co, Fe, or Co/Fe.

These findings are similar in some ways but significantly different in other ways compared with the results reported by Wu et al. for bulk PANI-derived bulk carbons (i.e., not mesoporous PANI nor mesoporous carbon).<sup>9</sup> On one hand, the electrocatalytic performance of our PDMCs containing metals toward ORR was comparable to those of the carbon materials reported by Wu et al. On the other hand, in the case of Wu et al., higher electrocatalytic activity of the carbon materials was obtained only when the materials had cobalt or iron in them; interestingly, however, in our case, the strongest electrocatalytic activity was obtained when the PDMC had no metal dopants at all. This unprecedented result begged for more information about the compositions of the PDMC materials to which this effect could be attributed.

Thus, chemical surface analysis of the PDMCs was performed using XPS (Figures S19–S24). The results suggested that the different nitrogen species depicted in Figure 2a were present in the PDMCs. Moreover, the N:C atomic ratio versus pyrolysis temperature plots of the samples (Figure 2b) showed that the N:C atomic ratio decreased significantly when the pyrolysis temperature was increased from 600 to 800 °C, but remained virtually unchanged when the pyrolysis temperature was increased from 800 to 900 °C, with N:C values of 4.30 and 4.39%, respectively.

Figure 2c graphs the percentage of different N species in the samples (determined from high-resolution N1s peaks on XPS) versus the pyrolysis temperature used to make the samples. First, when combined with the data obtained from Figure 1d, Figure 2c reveals a correlation between the quaternary N species and the ORR electron transfer number of PDMCs; i.e., whereas the PDMCs containing lower proportions of quaternary (graphitic) nitrogen species favor the two-electron process, those containing higher proportions of quaternary N centers favor the four-

electron process in ORR. Second, although quaternary and pyridinic species are generally the most stable phases at high temperatures (>600 °C) in N-doped carbon,<sup>15</sup> the pyrrolic/pyridone species were found to be the prominent N species in our case, especially in those PDMC samples obtained at 700 and 800 °C. [Note that, as the pyrrolic and pyridone nitrogens have very close N 1s XPS peaks, they are often considered indistinguishable.<sup>16</sup>] Most importantly, it is worth emphasizing that the pyrrolic N species in the PDMCs resemble the N groups in porphyrin-like structures, which were previously identified to be more active sites for ORR reaction.<sup>17</sup> In addition, the pyridone species, which can undergo tautomerization with hydroxypyridine (as shown in Figure S25), are known to stabilize singlet dioxygen by forming a stable adduct, as illustrated in Figure S26. The formation of such a stable adduct between pyridone and molecular oxygen has an oxygen chemisorption geometry analogous to the one verified for molecular oxygen adsorbed on Pt surfaces.<sup>18</sup> Therefore, the co-presence of the N and O species we identified on the graphitic structure of PDMC and the possible adduct formation between dioxygen and the pyridone groups on the PDMCs might have been, at least in part, responsible for the higher catalytic activity toward ORR exhibited by the metal-free PDMC. This proposed synergistic effect between N and O groups was further supported by analyzing the high-resolution C 1S XPS spectra for PDMC samples obtained at different pyrolysis temperatures (Figure 2d). When higher pyrolysis temperatures were used, the peak corresponding to (or the relative amount of) C atoms not directly linked to N and O atoms became lower. As the %N in the samples also decreased, reaching a minimum value of 4% (see above), as the pyrolysis temperature was increased, the relative amount of O species directly bonded to the C atoms must have increased. In fact, the relative amount of C atoms attached to O and N atoms in the samples reached a maximum value of >30% (with respect to all the C atoms) in the sample obtained at 800 °C (Figure 2d). Since the %N was only ca. 4%, this result indicated that this sample was composed largely of C–OH groups, many of which can be in the vicinity of the N centers and therefore can participate in the pyridine↔hydroxypyridine tautomerization discussed above. The source of the O species in the PDMCs could only be the mesoporous silica, as the carbonization was performed under an inert atmosphere, and the implantation of the O species from the silica into the PDMC may have been driven by the high temperature. The possible role of the O species present in PDMC on the PDMC's catalytic activity could also be implied on the basis of comparison of our result with the related bulk PANI-derived carbons devoid of oxygen dopants.<sup>17</sup>

In summary, the synthesis of novel N- and O-doped mesoporous carbon that showed efficient and stable electrocatalytic activity toward ORR is reported. The material was synthesized by pyrolysis of PANI/SBA-15 composite material, which was obtained by polymerization of PANI *in situ* within the pores of SBA-15 mesoporous silica. By doping the PANI/SBA-15 with different metal ions, the corresponding metal-containing PDMCs were also obtained. These materials also showed good activities toward ORR, albeit lower than that of the metal-free PDMC, challenging conventional paradigms. The unprecedented high electrocatalytic activity exhibited by the metal-free PDMC was attributed to the synergistic effect of the O and N species that were present as dopants on the materials and formed during pyrolysis. The synthetic method can easily be extended to other polymers or other metal oxides as template.

## ■ ASSOCIATED CONTENT

### 📄 Supporting Information

Detailed experimental procedure, description of electrochemical tests, and characterization results. This material is available free of charge via the Internet at <http://pubs.acs.org>.

## ■ AUTHOR INFORMATION

### Corresponding Author

tasefa@rci.rutgers.edu

### Notes

The authors declare no competing financial interest.

## ■ ACKNOWLEDGMENTS

T.A. gratefully acknowledges the financial assistance provided to his group by the U.S. National Science Foundation (grants DMR-0968937, CBET-1134289, NSF-ACIF, and NSF Special Creativity grant in 2011). R.S. acknowledges the CAPES in Brazil and the Fulbright Agency in the U.S. for graduate fellowships.

## ■ REFERENCES

- (1) Reddington, E.; Sapienza, A.; Gurau, B.; Viswantaan, R.; Sarangapani, S.; Smotkin, E. S.; Mallouk, T. E. *Science* **1998**, *280*, 1735.
- (2) (a) Nørskov, J. K.; Rossmeisl, J.; Logadottir, A.; Lindqvist, L.; Kitchin, J. R.; Bligaard, T.; Jonsson, H. *J. Phys. Chem. B* **2004**, *108*, 17886. (b) Ji, X.; Lee, K. T.; Holden, R.; Zhang, L.; Zhang, J.; Botton, G. A.; Couillard, M.; Nazari, L. F. *Nat. Chem.* **2010**, *2*, 286.
- (3) (a) Gong, K.; Du, F.; Xia, Z.; Durstock, M.; Dai, L. *Science* **2009**, *323*, 760. (b) Chen, S.; Bi, J.; Zhao, Y.; Yang, L.; Zhang, C.; Ma, Y.; Wu, Q.; Wang, X.; Hu, Z. *Adv. Mater.* **2012**, *24*, 5593. (c) Li, H.; Liu, H.; Jong, Z.; Qu, W.; Geng, D.; Sun, X.; Wang, H. *Int. J. Hydrogen Energy* **2011**, *36*, 2258.
- (4) (a) Zhao, Y.; Yang, L.; Chen, S.; Wang, X.; Ma, Y.; Wu, Q.; Jiang, Y.; Qian, W.; Hu, Z. *J. Am. Chem. Soc.* **2013**, *135*, 1201. (b) Wang, S.; Zhang, L.; Xia, Z.; Roy, A.; Chang, D. W.; Baek, J.-B.; Dai, L. *Angew. Chem., Int. Ed.* **2012**, *51*, 4209.
- (5) (a) Lefèvre, M.; Dodelet, J. P.; Bertrand, P. *J. Phys. Chem. B* **2000**, *104*, 11238. (b) Sawai, K.; Suzuki, N. *J. Electrochem. Soc.* **2004**, *151*, A682. (c) Lefèvre, M.; Proietti, E.; Jaouen, F.; Dodelet, J. P. *Science* **2009**, *324*, 71. (d) Kothandaraman, R.; Nallathambi, V.; Artyushkova, K.; Barton, S. C. *Appl. Catal. B: Environ.* **2009**, *92*, 209.
- (6) (a) Subramanian, N. P.; Li, X.; Nallathambi, V.; Kumaraguru, S. P.; Colon-Mercado, H.; Wu, G.; Lee, J.-W.; Popov, B. N. *J. Power Sources* **2009**, *188*, 38. (b) Kundu, S.; Nagaiah, T. C.; Xia, W.; Wang, Y.; Dommele, S. V.; Bitter, J. H.; Santa, M.; Grundmeier, G.; Bron, M.; Schuhmann, W.; Muhler, M. *J. Phys. Chem. C* **2009**, *113*, 14302.
- (7) Wang, B. *J. Power Sources* **2005**, *152*, 1.
- (8) Silva, R.; Asefa, T. *Adv. Mater.* **2012**, *24*, 1878.
- (9) Wu, G.; More, K. L.; Johnston, C. M.; Zelenay, P. *Science* **2011**, *332*, 443.
- (10) Wu, G.; Mack, N. H.; Gao, W.; Ma, S.; Zhong, R.; Han, J.; Baldwin, J. K.; Zelenay, P. *ACS Nano* **2012**, *6*, 9764.
- (11) Gavrilov, N.; Pašti, I. A.; Mitrić, M.; Trivas-Sejdić, J.; Ćirić-Marjanović, G.; Mentus, S. V. *J. Power Sources* **2012**, *220*, 306.
- (12) (a) Johnson, S. A.; Ollivier, P. J.; Mallouk, T. E. *Science* **1999**, *283*, 963. (b) Ding, S.; Zheng, S.; Xie, M.; Peng, L.; Guo, X.; Ding, W. *Microporous Mesoporous Mater.* **2011**, *142*, 609.
- (13) Fellingner, T.-P.; Hasché, F.; Strasser, P.; Antonietti, M. *J. Am. Chem. Soc.* **2012**, *134*, 4072.
- (14) Wang, H.; Maiyalagan, T.; Wang, X. *ACS Catal.* **2012**, *2*, 781.
- (15) Matter, P. H.; Zhang, L.; Ozkan, U. S. *J. Catal.* **2006**, *239*, 83.
- (16) Pels, J. R.; Kapteijn, F.; Moulijn, J. A.; Zhu, Q.; Thomas, K. M. *Carbon* **1995**, *33*, 1641.
- (17) Wu, G.; Chen, Z.; Artyushkova, K.; Garzon, F. H.; Zelenay, P. *ECSS Trans.* **2008**, *16*, 159.
- (18) Balbuena, P. B.; Altomare, D.; Agapito, L.; Seminario, J. M. *J. Phys. Chem. B* **2003**, *107*, 13671.